Vol 14 No 5, May 2005
1009-1963/2005/14(05)/1055-05

Chinese Physics

© 2005 Chin. Phys. Soc.
and IOP Publishing Ltd

Effects of grain size distribution on remanence and coercivity of $Pr_2Fe_{14}B$ nanocrystalline magnet*

He Shu-Li(贺淑莉)[a)b)], Zhang Hong-Wei(张宏伟)[a)†], Rong Chuan-Bing(荣传兵)[a)], Chen Ren-Jie(陈仁杰)[a)], and Shen Bao-Gen(沈保根)[a)]

[a)] *State Key Laboratory of Magnetism, Institute of Physics and Centre for Condensed Matter Physics, Chinese Academy of Sciences, Beijing* 100080, *China*

[b)] *Department of Physics, Capital Normal University, Beijing* 100037, *China*

(Received 30 November 2004; revised manuscript received 19 January 2005)

The demagnetization curves of $Pr_2Fe_{14}B$ nanocrystalline magnets are calculated using micromagnetic finite-element method. Samples with three different distributions of grain size are simulated. We find that the remanence enhancement does not depend on grain size distribution but on the mean diameter of grains, and the influence of grain size distribution on coercivity is affected by the strength of intergrain exchange coupling.

Keywords: nanocrystalline magnets, coercivity, remanence
PACC: 7560E, 7550V

1. Introduction

Nanocrystalline permanent magnets (NPMs) have attracted considerable interest because of their low rare-earth content and relatively high maximum energy production $(BH)_{max}$.[1−5] The remanence enhancement, which is due to the intergrain exchange coupling (IGEC) in isotropic NPMs, results in the high $(BH)_{max}$. Therefore, IGEC plays an important role in NPMs, after the grain size reduced to nanoscale.[6,7] Many efforts have been made to understand the effects of grain size on coercivity and remanence. However, due to the limitation of experimental technology, the effects of grain distribution on the magnetic properties in NPMs were scarcely investigated. Fortunately, the influence of grain size distribution on the magnetic properties can be investigated by finite element method (FEM) based on micromagnetics. Up to now, numerous calculations using micromagnetic FEM have been made on NPMs.[8−14] The simulation results are in good agreement with the experimental data. In this paper, the relationship between the grain size distribution and magnetic properties for isotropic NPMs is investigated using micromagnetic FEM.

2. Simulation model

The numerical simulation model to investigate magnetization processes in ferromagnetics is based on the continuum theory of micromagnetics. By means of FEM, the total magnetic Gibbs free energy,

$$G = E_{\rm H} + E_{\rm D} + E_{\rm k} + E_{\rm ex},$$

is minimized with respect to the direction of the spontaneous polarization $J_{\rm s}$. Here, $E_{\rm H}$ is the Zeeman energy in an external field, $E_{\rm D}$ the dipolar interaction energy, $E_{\rm k}$ the anisotropy energy and $E_{\rm ex}$ the exchange energy. In numerical calculations, dipolar interaction, which is neglected in Refs.[15,16], is taken into consideration by introducing a magnetic vector potential. A more detailed description of the simulation method used has been given in Ref.[17].

The samples consisting of 125 irregular grains were simulated, as shown in Fig.1. Figure 2 describes three different distributions of grain sizes. Distribution A shows a narrower distribution of grain size diameters than distributions B and C. Distributions B and C show the same range of grain sizes, but the details of their grain size distribution are different. Distribution C shows two characteristic maxima in the grain size distribution, which is similar to that of

*Project supported by the National Natural Science Foundation of China (Grant No 10274102).
†E-mail: hwzhang@g203.iphy.ac.cn

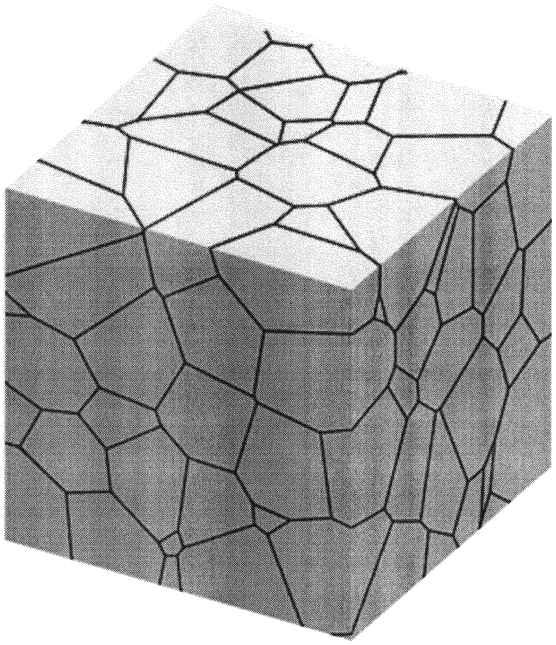


Fig.1. Schematic diagram of the sample composed of 125 irregular shaped grains.

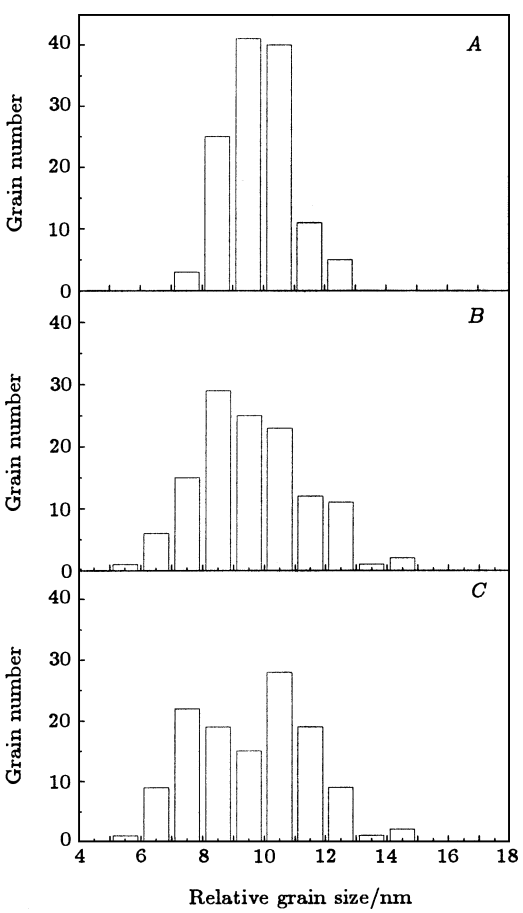


Fig.2. Distribution of grain sizes for the simulated samples, relative grain size= (grain diameter/mean diameter) $\times$10nm.

nanocomposite magnets. We aim to study the magnetic properties of the single-phase magnets that exhibit the same grain size distribution as the nanocomposite magnets. The mean diameter of the grain sizes (d) varies from 3 to 30nm, and the directions of the easy axes are distributed isotropically. For numerical simulations, the following material parameters of $Pr_2Fe_{14}B$ at room temperature are used: J_s=1.569T, K_1=5.567$\times10^6$J/m^3, and A=7.7$\times10^{-12}$J/m. Thus, the Bloch domain wall width is δ_B=3.7nm and the anisotropy field is $\mu_0 H_A$=8.9T. In calculations, 75000–95000 elements are used.

3. Results and discussion

3.1. Remanence

Figure 3 gives the grain diameter dependence of reduced remanence $m_r(=J_r/J_s)$. In the noninteracting Stoner–Wohlfarth model, m_r is expected to be 0.5. As shown in Fig.3, remanence enhancement is clearly observed for the samples with three different distributions of grain sizes. In NPMs, the increase of surface ratio can cause the strong IGEC. IGEC forces magnetization to deviate somewhat from the local easy axis, which leads to a smooth rotation of the magnetization vector from easy-axis orientation of a grain to that of the neighbour. This brings about the decrease of demagnetization effect and results in the remanence enhancement. The width of the exchange coupling area is approximately equal to δ_B. The volume ratio of the exchange coupling area is enhanced with decreasing grain size. So, the remanence enhancement effect becomes more remarkable for the sample with smaller grains, which is in good agreement with the result in Fig.3. Furthermore, no significant difference in remanence for the samples with different grain size distributions can be found. As discussed above, the

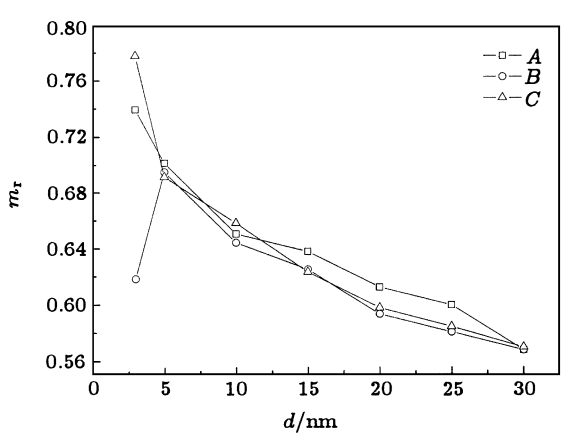


Fig.3. Dependence of reduced remanence m_r on mean grain size d.

volume ratio of exchange coupling which leads to the remanence enhancement is mainly controlled by the mean grain size instead of the size distribution. Therefore, remanence enhancement does not depend on the size distribution but on the mean grain size.

For samples with A and C distributions, m_r decreases with the grain size varying from 3 to 30nm. For samples with B distribution, m_r increases with decreasing grain size and exhibits a maximum when grain size is of 5nm, then reduces with grain size reduced to 3nm. This phenomenon reminds us of the necessity to investigate the demagnetization behaviour of the samples. Figure 4 shows the part of demagnetization curve at the field around zero for three samples with d=3nm. It is clearly seen that a sudden drop of magnetization happens before the applied field decreases to zero for the sample with B distribution. The sudden drop of magnetization can be reasonably related to the small remanence and is suggested to be the discontinuous change of magnetic moment directions in some local areas in the sample. Figures 5(a) and 5(b) describe the magnetization vector of samples with B distribution at the points E and F (indicated in Fig.4) respectively. The sudden drop of magnetization is caused by the rotating of the magnetization vectors in some grains as shown in the Fig.5. For the sample with grains of a few nanometers, enhancing exchange coupling results in the high-energy state of the system. Because of the stray field, the magnetization vector in the grains whose local easy axis is at a large angle with the direction of the applied field will rotate to lower E_{ex} of the system. It means that the dipolar interaction cannot be neglected in the sample with grains of several nanometers. In our numerical calculation, dipolar interaction is taken into consideration. However, dipolar interaction was not considered in Refs.[15,16]. As the mean grain size in their simulated samples is larger than 10nm, the dipolar interaction can be neglected and their results are reliable. Although the problem of dipolar interaction is very complicated,[18,19] it results in the decline of remanence in NPMs.[20] Therefore, the drop of m_r for the sample with B distribution can be attributed to the effect of dipolar interaction on remanence.

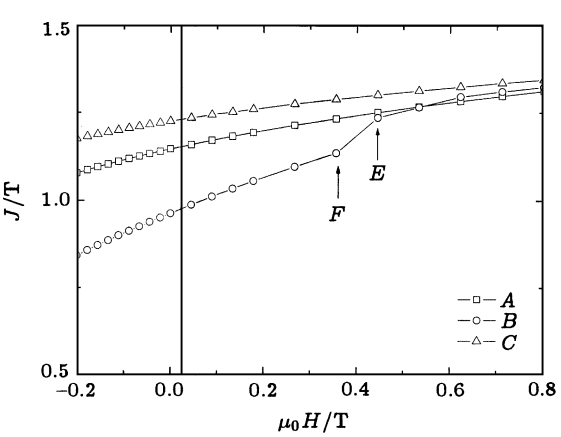


Fig.4. Demagnetization curves of the samples with d=3nm around zero applied field.

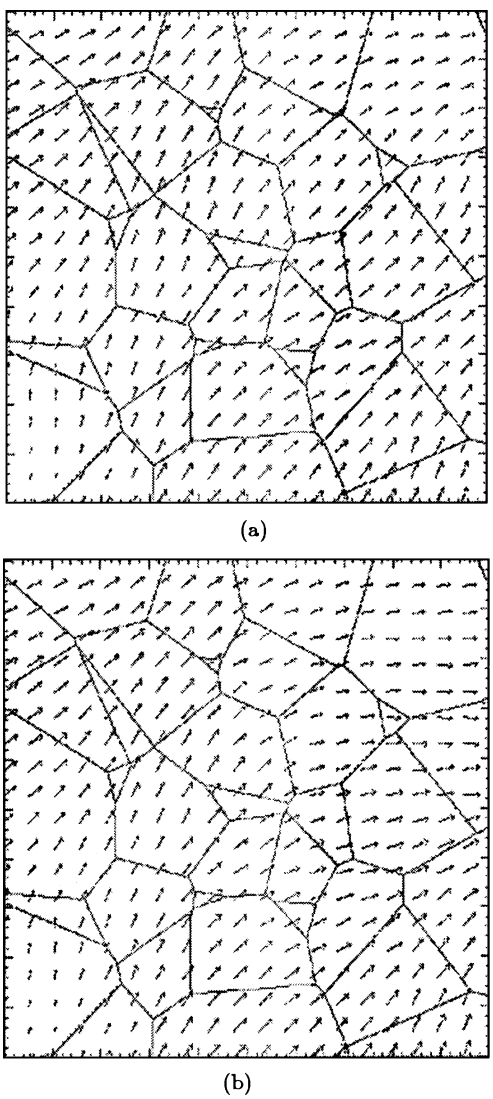


Fig.5. Magnetization vector of sample with A distribution (d=3nm) at point E (a) and point F (b) indicated in Fig.4.

3.2. Coercivity

Coercivity is sensitive to the microstructure of the sample. Figure 6 shows the curve of H_c versus d for three different kinds of samples. H_c drops monotonically with decreasing d. In NPMs, IGEC not only leads to remanence enhancement, but also results in the reduction of nucleation field. The competition

between anisotropy and IGEC makes the magnetization in the grain boundary deviate from the local easy axis. Thus, the magnetization in the grain boundary reverses more easily than that in the grain centre. The area fraction of exchange coupling enhances with decreasing d. Especially, when d approaches to $2\delta_B$, it increases rapidly. From Fig.6, it can be seen that H_c drops sharply when d is smaller than 8nm. For d=3nm, coercivities of the samples with A, B and C distributions are 0.69, 0.45 and 0.58T respectively. For d=5nm, H_c of the three kinds of samples are 1.31, 1.02 and 1.14T respectively. For $d \leq 5$nm, H_c of the sample with A distribution increases by about 15 percent compared with that of the sample with C distribution, and H_c of the sample with C distribution increases by about 20 percent compared with that of the sample with B distribution. For $d > 5$nm, no significant difference of H_c can be found among the samples with the three kinds of distributions as shown in Fig.6. In the process of demagnetization, as the stray field energy has been greatly released at around zero field, which results in the weak dipolar interaction in the system. It means that the influence of dipolar interaction on H_c can be neglected compared with other energies.

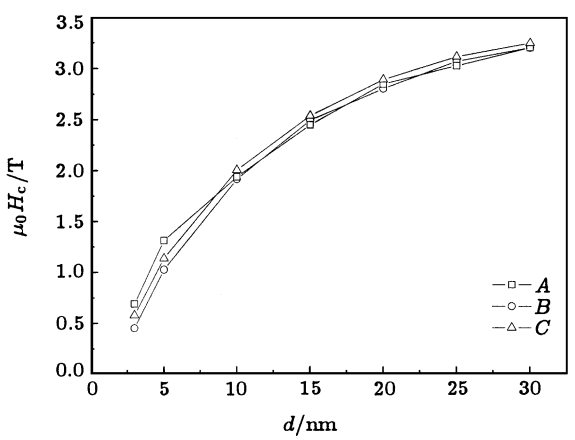


Fig.6. Dependence of coercivity H_c on mean grain size d.

More details in the demagnetizing process may be obtained from their demagnetization curves. Figure 7 shows the demagnetization curve of the samples with d=3nm. As shown in Fig.7, the magnetization of the samples with A and B distributions reverses in a lump, and the magnetization of the sample with C distribution reverses by stages. Figures 8(a) and 8(b) are the magnetization vector of the sample with C distribution at points G and H (indicated in Fig.7) respectively. It can be observed that the magnetization vector in larger grains rotates a large angle. The data of energy calculation show that the rotation of

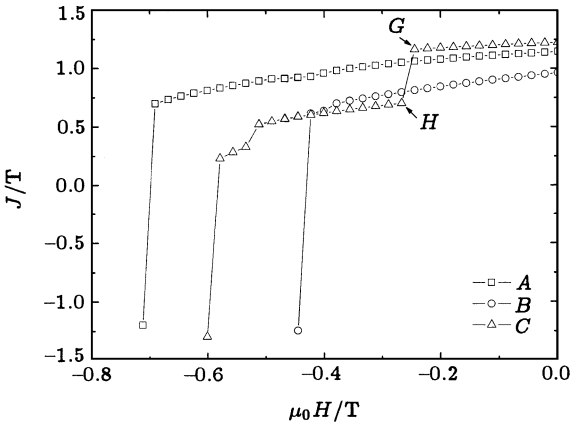


Fig.7. Demagnetization curves of the samples with d=3nm.

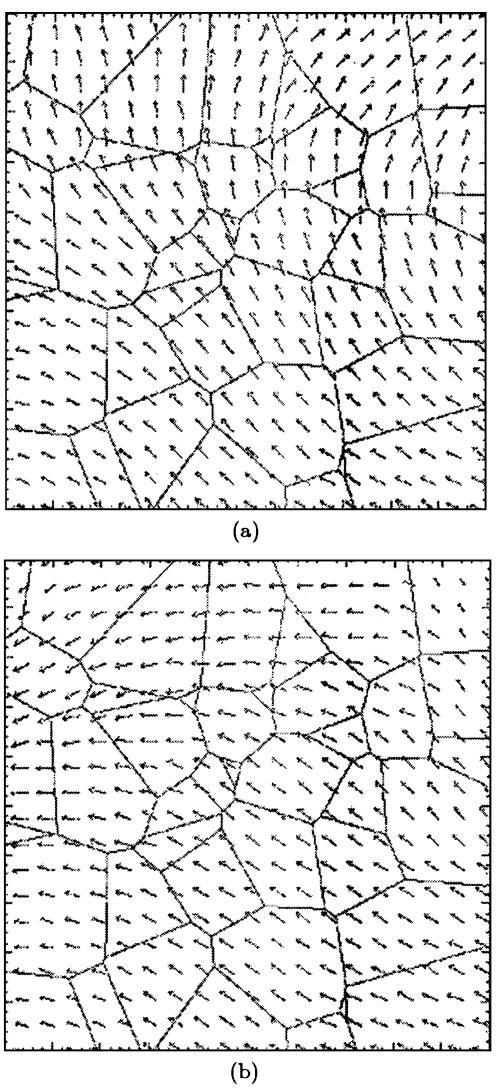


Fig.8. Magnetization vector of the sample with C distribution (d=3nm) at points G (a) and H (b) which are indicated in Fig.7.

magnetization vector in large grains not only leads to the increase of E_{ex}, but also results in a dramatic decrease of E_H, which brings about the reduction of energy in the sample with C distribution. For the sample with A distribution, due to the lack of large grains, the rotation of magnetization vector will result in the increase of E_{ex} and the slight decrease of E_H, which will not lead to the decrease of total energy in the system.

Although IGEC is very strong in all three kinds of samples, the contribution of IGEC to the anti-reverse in large grains is weak. Therefore, the magnetization vector in large grains can reverse under a relative low field, which would lead to the decrease of H_c. For $d \geq$ 10nm, as IGEC is weakened, the influence of grain size distribution on H_c becomes less important.

4. Conclusions

(1) There is no significant difference in remanence for the samples with different distributions of grain sizes. Remanence enhancement does not depend on the grain size distribution but on the mean diameter of grain sizes.

(2) For mean diameter d being several nanometers, obvious difference can be found among the samples with three different kinds of distributions. For $d \geq$10nm, the grain size distribution has hardly influence on H_c of the samples.

References

[1] Hadjipanayis G C, Hazelton R C and Lawless K R 1983 *Appl. Phys. Lett.* **43** 797

[2] Croat J J, Herbst J F, Lee R W and Pinkerton F E 1984 *J. Appl. Phys.* **55** 2078

[3] Wecker J, Schnitake K, Cerva H and Grogger W 1995 *Appl. Phys. Lett.* **67** 563

[4] Goll D, Seeger M and Kronmuller H 1998 *J. Magn. Magn. Mater.* **185** 49

[5] Hadjipanayis G C 1999 *J. Magn. Magn. Mater.* **200** 373

[6] Hadjipanayis G C and Gong W 1988 *J. Appl. Phys.* **64** 5559

[7] Manaf A, Buckley R A, Davies H A and Leonowicz M 1991 *J. Magn. Magn. Mater.* **101** 360

[8] Fischer R, Leineweber T and Kronmuller H 1998 *Phys. Rev.* B **57** 10723

[9] Kronmuller H, Fischer R, Bachmann M and Leineweber T 1999 *J. Magn. Magn. Mater.* **203** 12

[10] Zhao S F, Jin H M, Wang X F and Yan Y 2001 *Chin. Phys.* **10** 1157

[11] Zhang H W, Rong C B, Du X B, Zhang S Y and Shen B G 2004 *J. Magn. Magn. Mater.* **278** 127

[12] Rong C B, Zhang H W, Du X B, Zhang J, Zhang S Y and Shen B G 2004 *J. Magn. Magn. Mater.* **277** 221

[13] Zhang H W, Rong C B, Zhang J, Zhang S Y and Shen B G 2003 *Acta Phys. Sin.* **52** 718 (in Chinese)

[14] Rong C B, Zhang H W, Zhang J, Zhang S Y and Shen B G 2003 *Acta Phys. Sin.* **52** 708 (in Chinese)

[15] Griffiths M K, Bishop J E L, Tucker J W and Davies H A 1998 *J. Magn. Magn. Mater.* **183** 49

[16] Jin H M, Kim Y B and Wang X F 1998 *J. Phys.: Condens. Matter* **10** 7243

[17] Fischer R and Kronmuller H 1996 *Phys. Rev.* B **54** 7284

[18] Kechrakos D and Trohidou K N 1998 *Phys. Rev.* B **58** 12169

[19] Morup S, Bodker F, Hendriksen P V and Linderoth S 1995 *Phys. Rev.* B **52** 287

[20] Kronmuller H, Fischer R, Seeger M and Zern A 1996 *J. Phys.* D: *Appl. Phys.* **29** 2274